

CO⁺ in M 82: A Consequence of Irradiation by X-rays

M. Spaans

Kapteyn Astronomical Institute, P.O. Box 800, 9700 AV Groningen, The Netherlands

spaans@astro.rug.nl

and

R. Meijerink

Astronomy Department, University of California, Berkeley, CA 94720, United States

rowin@astro.berkeley.edu

ABSTRACT

Based on its strong CO⁺ emission it is argued that the M 82 star-burst galaxy is exposed to a combination of FUV and X-ray radiation. The latter is likely to be the result of the star-burst superwind, which leads to diffuse thermal emission at ~ 0.7 keV, and a compact hard, 2-10 keV, source (but not an AGN). Although a photon-dominated region (FUV) component is clearly present in the nucleus of M 82, and capable of forming CO⁺, only X-ray irradiated gas of density $10^3 - 10^5$ cm⁻³ can reproduce the large, $\sim (1 - 4) \times 10^{13}$ cm⁻², columns of CO⁺ that are observed toward the proto-typical star-burst M 82. The total X-ray luminosity produced by M 82 is weak, $\sim 10^{41}$ erg s⁻¹, but this is sufficient to drive the formation of CO⁺.

Subject headings: X-rays: ISM — X-rays: galaxies — ISM: molecules — galaxies: starburst

1. Introduction

M 82 is a star-burst galaxy located at 3.9 Mpc (Sakai & Madore, 1999). It has a bolometric luminosity of $\sim 4 \times 10^{10}$ L_⊙ and a large body of observational data exists for this system. The observed X-ray luminosity of M 82 is modest at $\sim 4 \times 10^{40}$ erg s⁻¹ and ROSAT and ASCA data indicate that it has a hard, strongly absorbed ($N_H \sim 10^{22}$ cm⁻²) power-law component and diffuse thermal contributions at $kT \approx 0.6$ and 0.3 keV (Moran

& Lehnert 1997). More recent XMM observations indicate a range of temperatures from 0.2-1.6 keV, peaking at 0.7 keV, for the diffuse thermal component (Read & Stevens 2002). The thermal contributions result from the star-burst superwind and the star formation itself (supernova heating of the ISM). There is a compact hard (2-10 keV) X-ray component that is absorbed with a photon index of 1.7 in the nucleus M 82, and that varies on a 62 days period (Kaaret, Simet & Lang 2006a,b). There is a modest, 4.4×10^{39} erg s⁻¹, 2-8 keV diffuse component (Strickland & Heckman 2007). The work of Moran & Lehnert (1997) argues that the intrinsic luminosity of M 82 in the 0.1-10 keV band is about four times larger when absorption is properly taken into account, yielding about 10^{41} erg s⁻¹ in total. The CO⁺ chemistry presented here is most sensitive to the softer diffuse thermal component (which is largely absorbed for our model clouds), so subtleties in the hard 2-10 keV band do not impact the presented results. There is no clear evidence of an AGN (i.e., a buried Seyfert nucleus) in M 82. The X-ray luminosity is about $\sim 0.2\%$ of the total FUV energy budget as measured by the FIR luminosity (Pak et al. 2004).

In the center of the late-type galaxy M 82, bright (and optically thin) CO⁺ N=2-1, J=5/2-3/2 (236.06 GHz) and J=3/2-1/2 (235.79 GHz) rotational emission has been observed by Fuente et al. (2006). Based on combined CN and HCO⁺ measurements (their Figure 2 and Table 2), the latter authors argue for a clumpy photon-dominated region (PDR) model where $\sim 4 \times 10^5$ cm⁻³ clumps are embedded in an inter-clump medium and are exposed to an enhancement in the FUV radiation field of $G_0 \sim 10^4$. This enhancement is with respect to the average far-ultraviolet (6-13.6 eV) instellar radiation field in the Milky Way, which enjoys a typical FUV flux of 1.6×10^{-3} erg s⁻¹ cm⁻². It is certainly established that FUV photons produced by the vigorous star formation in M 82 dominate the state of the molecular gas in its center (e.g., Pak et al. 2004 and references therein for ro-vibrational H₂ as well as [CII] and [OI] fine-structure emission), and observations of CO, HCO⁺ and CN can be explained as well by a PDR interpretation. However, CO⁺ is under-abundant by at least an order of magnitude in such PDR models, compared to the observed CO⁺ columns of $\sim (1 - 4) \times 10^{13}$ cm⁻² (Fuente et al. 2006).

In this letter, we investigate whether the large CO⁺ columns measured toward M 82 by Fuente et al. (2006) can be explained by the irradiation of molecular gas by the modest X-ray component that M 82 exhibits, without violating the clear merits of PDR physics.

2. PDR and XDR models

We have constructed a set of PDR and X-ray Dominated Region (XDR) models from the codes described by Meijerink & Spaans (2005), Meijerink, Spaans & Israel (2006) and

Meijerink, Spaans & Israel (2007) in which we vary both the incident radiation field, density and cosmic-ray ionization rate. The thermal balance (with line transfer) is calculated self-consistently with the chemical balance through iteration. Absorption cross sections for X-rays are smaller, $\sim 1/E^3$, than for FUV photons. Therefore, PDRs show a stratified structure while the changes in the chemical and thermal structure in XDRs are very gradual. In XDRs, additional reactions for fast electrons that ionize, excite and heat the gas are included. The heating efficiency in XDRs is much higher. Since we focus on galaxy centers, we have assumed the metallicity to be twice Solar. We take the abundance of carbon to be equal to that of oxygen, since the carbon abundance increases faster than oxygen for larger metallicity. The precise C:O ratio does not affect our general results, with the exception of O₂ and H₂O abundances (Bergin et al. 2000, Spaans & van Dishoeck 2001). Because the metallicity, even for a system like M 82, is generally poorly known in the central regions of active star formation, we have also run models with Solar metallicity. We come back to these in the discussion section.

Our models (Meijerink et al. 2007) have $n = 10^2 - 10^{6.5} \text{ cm}^{-3}$ and $G_0 = 10^1 - 10^5$ ($F_X = 0.01 - 160 \text{ erg s}^{-1} \text{ cm}^{-2}$). We adopt a standard size for our model clouds of 1 or 10 pc. Our X-ray spectrum follows the spectral characteristics observed for M 82, corrected for extinction by the observed hydrogen column density ($\sim 10^{22} \text{ cm}^{-2}$). This attenuation is important (factor of four) and is the reason why the total X-ray luminosity is about $10^{41} \text{ erg s}^{-1}$ (see introduction). The X-ray spectral shape matters a lot for the penetration of photons in particular energy bands. Still, for the case of M 82, molecular ion formation is not very sensitive to the exact spectrum. Overall most of the M 82 X-ray energy is emitted below a few keV. Now, a purely soft spectrum would be absorbed quickly in the outer layers of the XDR, while a purely hard spectrum would penetrate all the way through. But to first order it is the total energy deposition rate, basically the integral of the absorbed flux, that drives the chemistry (Meijerink & Spaans 2005). Our model clouds, with $N_H \sim 10^{22} \text{ cm}^{-2}$ per cloud, are chosen such that they absorb the bulk of the diffuse thermal X-ray flux of M 82, consistent with the significant absorption that the observations indicate, and thus the dependence on the exact X-ray spectral shape is modest as far as the produced column densities are concerned.

The considered densities and fluxes are representative of the conditions in M 82 in terms of PDRs, but only the models with $F_X \leq 10 \text{ erg s}^{-1} \text{ cm}^{-2}$ should be typical of the X-ray background in M 82. That is, a total X-ray luminosity of $10^{41} \text{ erg s}^{-1}$ yields $F_X \approx 0.4 \text{ erg s}^{-1} \text{ cm}^{-2}$ for a point source at 50 pc from a molecular cloud. We also consider larger values for F_X because the thermal X-ray emission is diffuse and molecular gas will enjoy a range of distances to ambient X-ray sources. For example, Fuente et al. (2006) adopt an emission size of $6''$ for CO⁺, corresponding to a linear scale of about 100 pc at the distance

to M 82. Imagine then that the interstellar medium of M 82 consists of a large number of ~ 1 -10 pc clouds. If some of these clouds are at distances of about 1 pc to individual sources of X-ray radiation, then only about 1% of the total X-ray luminosity per source would already yield $F_X \sim 10 \text{ erg s}^{-1} \text{ cm}^{-2}$ impinging on these clouds. At the same time can the covering factor of about a hundred of these clouds on the sky approach 5-50%, and thus contribute significantly to the XDR signal.

3. Results

Figure 1 shows the CO^+ column densities for a $n = 10^3 - 10^4 \text{ cm}^{-3}$ (10 pc cloud) and a $n = 10^4 - 10^{6.5} \text{ cm}^{-3}$ (1 pc cloud) density range. When comparing the model results with the observations, one should realize that the observed CO^+ column densities are actually determined for gas densities around 10^5 cm^{-3} and a rotational excitation temperature of about 10 K (Fuente et al. 2003). We also show lower density models in figure 1 because the excitation of CO^+ is quite complicated (Black 1998, Stauber et al. 2006). We come back to this point in the discussion. In table 1 an overview is given of all the relevant chemical species and their ratios.

It is obvious that XDRs allow columns of CO^+ that are comparable to the observed range of $\sim (1 - 4) \times 10^{13} \text{ cm}^{-2}$ for modest densities, while 10^5 cm^{-3} gas requires a few clouds to be superposed along the line of sight, which seems very reasonable. From the abundances shown in figure 2, where a comparison is made between a typical XDR and PDR model, it is evident that the CO^+ abundance is more than an order of magnitude enhanced for the same total impinging flux by energy. This is a direct consequence of the more significant $\text{C}^+ + \text{OH} \rightarrow \text{CO}^+ + \text{H}$ pathway in XDRs, where large amounts of C^+ and OH co-exist to large depths (Meijerink & Spaans 2005). Note in this that the endo-thermic $\text{O} + \text{H}_2 \rightarrow \text{OH} + \text{H}$ reaction is driven efficiently at the high ($\geq 100 \text{ K}$) gas temperatures that pertain in XDRs even at large columns (Meijerink & Spaans 2005), augmented by the vibrational excitation of H_2 . The XDR HOC^+ abundances are also much larger than in PDRs and the model column densities are comparable to those of CO^+ , consistent with observations. The XDR $\text{HCO}^+/\text{HOC}^+$ column density ratios are of the order of 20-40 when the total hydrogen column density is $\leq 10^{23} \text{ cm}^{-2}$, also consistent with observations (Fuente et al. 2006, their table 2).

Similarly, figure 2 and table 1 show that for column densities exceeding $10^{21.5} \text{ cm}^{-2}$ the CO^+/HCO^+ column density ratio reaches values of 0.01-0.1 in XDRs, and is boosted relative to PDRs for the same ambient density and total impinging flux by energy. Values of 0.01-0.1 can be reached for PDRs as well, but only if the columns are modest, $\leq 10^{21.5} \text{ cm}^{-2}$. All this compares well with the 4.5-6.5 mag range for individual clumps in the Fuente et al.

model. Our adopted cosmic-ray ionization rate is 5×10^{-15} comparable to the Fuente et al. value. We find (see also Meijerink et al. 2006) that a boost in the formation of CO^+ through an enhanced cosmic ray ionization rate does not occur because direct ionization of CO is negligible and the C^+ abundance is simply too small beyond the radical region in PDRs to react with OH.

Finally, in their model Fuente et al. (2006) require about 20-40 PDR clumps of $4 \times 10^5 \text{ cm}^{-3}$ density and 7 mag extinction in order to reproduce the observed CN column of $\sim 10^{16} \text{ cm}^{-2}$. Figure 2 shows that XDRs with low impinging X-ray fluxes do not exhibit strongly enhanced CN abundances (with large F_X they would), but have abundances similar to or somewhat smaller than PDRs. Table 1 shows that our PDR model with $G_0 = 10^{3.5}$ and $n = 10^5 \text{ cm}^{-3}$ produces a CN column of a few $\times 10^{15} \text{ cm}^{-2}$, and requires several clumps along the line of sight, consistent with the CO^+ requirement at that density. The impinging FUV flux of this PDR model is a factor of 10 below the best fit model of Fuente et al. (2005). The PDR CN/HCN column density ratios of about 4-7 are also consistent with observations (Fuente et al. 2006, their table 2). The XDR CN/HCN column density ratios are about 80-180. However, the HCN abundance in an XDR is not strongly boosted at all for low F_X (see also Lepp & Dalgarno 1996, their figure 3). Consequently, the PDR contribution will dominate the observed HCN (as well as CN) signal and no inconsistency arises. Our models do not experience the bi-stability effect, where a low and a high ionization phase co-exist through the interplay of H_3^+ , S^+ and O_2 (e.g. Boger & Sternberg 2006), because gas-grain neutralization is rapid.

4. Discussion

The CO^+ abundance in X-ray irradiated interstellar gas is boosted, relative to the FUV irradiation case. The star-burst galaxy M 82 appears to need only a modest flux of X-rays, consistent with observations, in order to reproduce the observed CO^+ column across its nuclear disk at a density of $10^3 - 10^5 \text{ cm}^{-3}$. We conjecture that other star-burst galaxies may experience similar effects.

The metallicity in the central regions of M 82 is poorly known. Read & Stevens (2002) find super-solar abundances for Mg and Si, but near-solar values for N, O and Fe). For comparison we have run models with Solar metallicity and the same density and irradiation conditions. It turns out that Solar metallicity lowers the abundance of CO^+ by about a factor of two to three for columns less than a few times 10^{22} cm^{-2} , while the difference is no more than $\sim 50\%$ for columns larger than a few times 10^{22} cm^{-2} . This is a direct consequence of the fact that a lower metallicity causes a lower absorption rate of X-rays and thus a larger

total column of material is needed to build up the same column of ionization driven species like CO+. Since the bulk of the M 82 X-rays is absorbed in our model, i.e. we have total hydrogen columns of more than $3 \times 10^{22} \text{ cm}^{-2}$ (a few clumps), the impact of metallicity variations is modest. Specifically, for Solar metallicity and a total hydrogen column density of $2.5 \times 10^{22} \text{ cm}^{-2}$ (~ 2 clumps) or $5 \times 10^{22} \text{ cm}^{-2}$ (~ 4 clumps) we find CO+ columns of $2 \times 10^{12} \text{ cm}^{-2}$ (a factor 2.7 lower) or $5 \times 10^{12} \text{ cm}^{-2}$ (a factor 1.5 lower), respectively.

It would be quite useful to have H, H₂ and electron collisional rate coefficients for CO+. Still, the situation for CO+ is quite special in that it is a ‘transient’ molecule (Black 1998), for which the destruction time is shorter than the time to reach collisional equilibrium. As a consequence, the excited state that the formation process leaves the CO+ molecule in, should be an integral part of the excitation analysis because inelastic collisions with H₂ may not be able to thermalize the CO+ levels. Indeed, if CO+ is formed in an excited state, then a low density, $n = 10^3 - 10^4 \text{ cm}^{-3}$, gas component as shown in figure 1 and table 1 can already lead to large CO+ emissivities because CO+ column densities increase with F_X/n .

We thank J.P. Pérez Beaufuits, J. Martín-Pintado and S. García-Burillo for stimulating discussions on XDR chemistry. We thank P. Kaaret for information on recent X-ray observations of M 82.

REFERENCES

- Bergin, E.A., Melnick, G.J., Stauffer, J.R., Ashby, M.L.N., et al. 2000, ApJ, 539, L129
- Black, J.H., 1998, in ”Chemistry and Physics of Molecules and Grains in Space. Faraday Discussions No. 109, p. 257
- Boger, G.I. & Sternberg, A., 2006, ApJ, 645, 314
- Fuente, A., Rodríguez-Franco, A., García-Burillo, S., Martín-Pintado, J., & Black, J.H., 2003, A&A, 406, 899
- Fuente, A., García-Burillo, S., Gerin, M., Teyssier, D., Usero, A., Rizzo, J.R., & de Vicente, P., 2005, ApJ, 619, L155
- Fuente, A., García-Burillo, S., Gerin, M., Rizzo, J.R., Usero, A., Teyssier, D., Roueff, E., & Le Bourlot, J., 2006, ApJ, 641, L1 05
- Kaaret, P., Simet, M.G., & Lang, C.C., 2006, ApJ, 646, 174

- Kaaret, P., Simet, M.G., & Lang, C.C., 2006, *Science*, 311, 491
- Lehnert, M.D., Heckman, T.D., & Weaver, K.A., 1999, *ApJ*, 523, 575
- Lepp, S. & Dalgarno, A., 1996, *A&A*, 306, L21
- Meijerink, R. & Spaans, M. 2005, *A&A*, 436, 397
- Meijerink, R., Spaans, M., & Israel, F. P. 2006, *ApJ*, 650, 103
- Meijerink, R., Spaans, M. & Israel, F.P., 2007, *A&A*, 461, 793
- Moran, E.C. & Lehnert, M.D., 1997, *ApJ*, 478, 172
- Pak, S., Jaffe, D.T., Stacey, G.J., Bradford, C.M., Klumpe, E.W., & Keller, L.D., 2004, *ApJ*, 609, 692
- Read, A.M. & Stevens, I.R., 2002, *MNRAS*, 335, L36
- Sakai, S. & Madore B.F., 1999, *ApJ* 526, 599
- Spaans, M. & van Dishoeck, E.F., 2001, *ApJ*, 548, L217
- Stäuber, P., Benz, A.O., Jørgensen, J.K., van Dishoeck, E.F., Doty, S.D., van der Tak, F.F.S., 2006, *astro-ph/0608393*
- Strickland, D.K. & Heckman, T.M., 2007, *ApJ*, 658, 258

Table 1: Column densities and column density ratios

N_{H}	$N(\text{CO}^+)$	$N(\text{HOC}^+)$	$N(\text{HCO}^+)$	$N(\text{CN})$	$N(\text{HCN})$	CO^+/HCO^+	$\text{HCO}^+/\text{HOC}^+$	CN/HCN
XDR: $n = 10^5 \text{ cm}^{-3}$ and $F_x = 5.1 \text{ erg s}^{-1} \text{ cm}^{-2}$								
1.0e22	3.0e12	3.3e12	4.3e13	1.1e15	6.0e12	0.07	13.2	181
2.0e22	4.8e12	5.0e12	1.6e14	2.7e15	2.8e13	0.03	31.5	95.4
3.0e22	5.7e12	5.9e12	2.7e14	4.7e15	5.9e13	0.02	46.4	78.9
XDR: $n = 10^{3.5} \text{ cm}^{-3}$ and $F_x = 1.6 \text{ erg s}^{-1} \text{ cm}^{-2}$								
3.0e22	1.2e12	5.7e11	1.5e12	5.2e13	3.2e10	0.8	2.6	1.6e3
6.0e22	8.3e12	6.9e12	3.7e13	5.1e14	9.4e11	0.2	5.4	543
9.1e22	1.8e13	1.5e13	1.3e14	1.5e15	3.8e12	0.14	8.5	400
PDR: $n = 10^5 \text{ cm}^{-3}$, $G_0 = 10^{3.5}$ and $\zeta = 5 \times 10^{15} \text{ s}^{-1}$								
1.0e22	1.6e10	1.0e10	2.8e14	2.3e15	3.5e14	5.6e-5	2.8e4	6.6
2.0e22	1.7e10	1.5e10	7.8e14	4.5e15	9.5e14	2.2e-5	5.2e4	4.7
3.0e22	1.9e10	2.0e10	1.3e15	6.7e15	1.6e15	1.4e-5	6.5e4	4.3

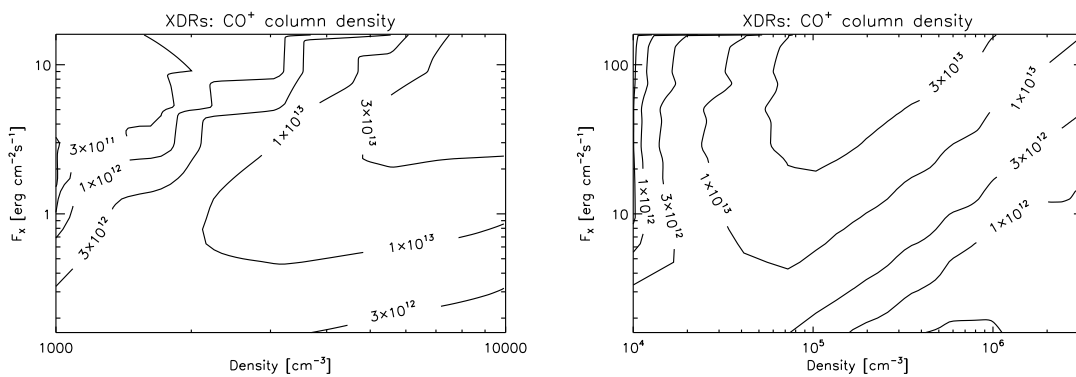


Fig. 1.— CO⁺ column densities in XDRs as derived from the models calculated in Meijerink et al. 2007. *Left:* Mid density range, $n = 10^3 - 10^4$ cm⁻³, and impinging fluxes of $F_X = 0.16 - 16$ erg s⁻¹ cm⁻². *Right:* High density range, $n = 10^4 - 10^{6.5}$ cm⁻³, and impinging fluxes of $F_X = 1.6 - 160$ erg s⁻¹ cm⁻².

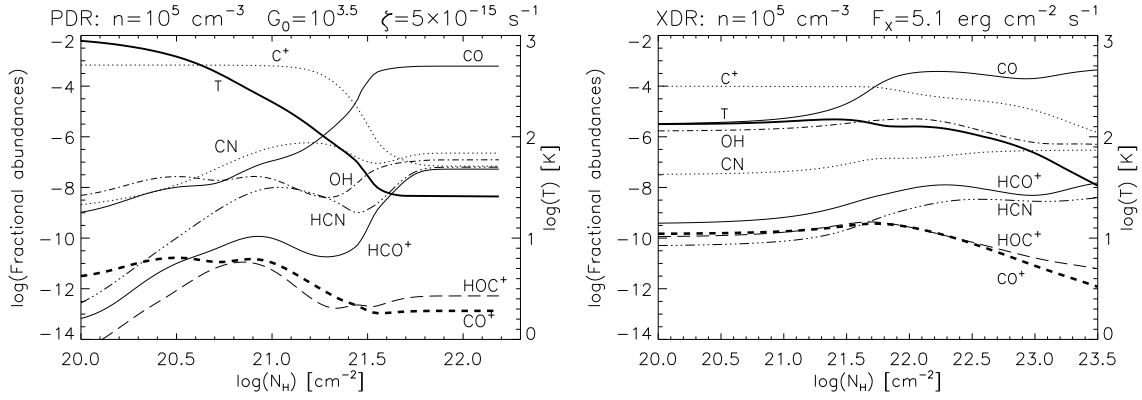


Fig. 2.— Chemical and thermal structure of a PDR with an enhanced cosmic ionization rate ($\zeta = 5 \times 10^{-15} \text{ s}^{-1}$) and an XDR model. Density $n = 10^5 \text{ cm}^{-3}$ and $G_0 = 10^{3.5}/F_X = 1.6 \text{ ergs s}^{-1} \text{ cm}^{-2}$. The CO^+ abundance is at least an order of magnitude larger in the XDR.